P7.6 A NEW APPROACH FOR ANALYZING AND COMPARING TRMM PR AND GROUND CP2 RADAR DATA FOR TWO CONVECTIVE STORMS NEAR BRISBANE, AUSTRALIA

Gwo-Jong Huang[1] and V.N. Bringi[1]

[1]Colorado State University, Fort Collins, Colorado, USA

1. INTRODUCTION

The TRMM precipitation radar (PR; K_u-band) on the Tropical Rainfall Measuring Mission (TRMM) satellite uses a hybrid method based on the Hitschfeld-Bordan (Hitschfeld and Bordan 1954) and the Surface Reference Technique (SRT; Meneghini et al. 2000) to do the attenuation-correction for the measured radar reflectivity. The basic assumptions for this method are, (*a*) a power-law relation between the specific attenuation (k) and measured radar reflectivity factor (Z_m) as $k=\alpha Z_m^{\beta}$, and (*b*) an assumption of three vertical models (stratiform rain with bright band, stratiform rain without bright band and convective rain, and others) for the initial α (α_{init}) and β (see Section 4 of Iguchi et al. 2000). With these assumptions, Iguchi et al. compute the path-integrated attenuation (referred to PIA_{HB}). At the same time, they also estimate independently *PIA* using SRT (referred to PIA_{SR}). By using these two *PIA*s into their statistical model, they evaluate an attenuation correction factor, namely ε_f in 2A25, and obtain the best estimate of the *PIA*. Although the DSD parameter retrievals are not part of the 2A25 products, the ε_f can be used to adjust α_{init} (α-adjustment procedure), and then relate to a constant N_w (normalized gamma intercept parameter) along the beam and varying D_0 (Ferriera et al. 2001; Chandrasekar et al. 2003).

The 2A25 vertical storm structure model in the mixed phase region is an important assumption along with the *k-Z* relations used. The term "mixed phase" refers to the supercooled rain drops mixed with wet graupel/hail hydrometeors in convection. While the bright band structure model is based on a firmer microphysical footing from previous studies (Awaka et al. 1985), the convective structure model, while developed for ocean events, may not be generally applicable for deeper convective land events where updrafts are stronger along with mixed phase precipitation starting as warm as 10° C and extending to -20℃. Moreover, the Hitschfeld-Bordan algorithm was mainly developed for correcting radar reflectivity in rain region only. Therefore, even assuming perfect *PIA* estimation, the α-adjustment procedure will cause an underestimation of N_w and correspondingly, overestimate D_0.

Figure 1: The map of Brisbane area. The CP-2 radar is located at "red +" and 2D-Video is at "yellow O".

The CP-2 radar which located to the SW of Brisbane (see Figure 1), Australia has been operated by Centre for Australian Weather and Climate Research in collaboration with NCAR since late 2007. This dual-wavelength/dual-polarization (S/X-band) radar, with its new signal processor developed at NCAR, can now measure the differential propagation phase (Φ_{dp}) and the copolar correlation coefficient (ρ_{hv}) at S-band. The original fields such as the dual-wavelength ratio *(DWR)*, *LDR* (at X-band), Z_{dr} (at S-band) and so on are still maintained. Moreover, the radar data quality evaluation was done by Bringi and Thurai (2008). Since this radar can directly measure *DWR* (difference between two measured radar reflectivity factors), we are able to compute the total specific

* Corresponding author address: Gwo-Jong Huang, Dept of Electrical Engr., Colorado State Uniiversity, Fort Collins, CO 80523; e-mail: gh222106@engr.colostate.edu

attenuation (k_{total}) independently from any assumptions of the microphysical properties of precipitation existing along the beam (Hubbert et al. 1995, Bringi et al 2009; these Conference proceedings 11A.3). With these unique features, we are able to use CP-2 radar (referred to GR) data to compare with the vertical profile of *k* from Version 6 using two overpass events near the Brisbane area.

In our approach, we first aligned and mapped GR and PR data set into a Cartesian coordinate system centered on the GR following Bolen and Chandrasekar (2003). To compare GR with PR, we mapped the GR-Z_h from S-band to K_u-band, and GR-*k* (computed from *DWR*) from X-band (9.4 GHz) to K_u-band. Next, we computed the GR-based path-integrated attenuation (*GR-PIA*), and used this *PIA* to correct the PR-measured reflectivity.

Here we compare data from two overpass storm events from the Brisbane area. One event was around 40 km off the coast, while the second was over land around 80 km to the NW (see Fig. 1).

2. FREQUENCY SCALING

Since the GR measurements are at S/X-band (2.8/9.4 GHz) and PR is at K_u-band (13.8 GHz), we have to frequency scale the GR data to K_u-band. We first assume linear relationships between Z_s and Z_{ku} (dBZ), and between k_x *and* k_{ku} (dB/km) as:

$$\begin{cases} Z_{ku} = a_1 Z_s + b_1 \\ k_{ku} = a_2 k_x + b_2 \end{cases} \quad \text{.....(1).}$$

To find the [a,b] parameters of these linear relationships, we need to simulate the radar observables. The simulations use the T-matrix technique and were done for 3 different hydrometeor types; namely, rain (dielectric constants at 0 and 20 ℃), wet ice (at 0 ℃), and snow (at -10 ℃). The 1-minute averaged DSDs used in the simulations were from 2008-2009 rainy season in Brisbane. The DSD data sets were measured by a 2D-Video disdrometer located NE of CP-2 (the yellow circle in Fig. 1). We note that since we are doing frequency scaling the DSD or particle SD parameter ranges are not as important as when the absolute *k* needs to be computed. The other assumptions using in simulations are as follows:

(a) Rain: raindrops are assumed to be modified conical shape (Thurai et al. 2007). The distribution of zenith angle (θ) is Gaussian with 7.5° standard deviation and zero mean. The distribution of azimuth angle (ϕ) is uniform in [0,2π].

(b) Wet ice: wet graupel/hail is assumed to be a spheroid with 0.8 axis ratio. The distribution of θ is Gaussian with σ_θ = 45° and zero mean. The ϕ is uniform in [0,2π]. The density of wet ice is 0.64 g cm^{-3} (mixture of 33% air, 33% water and 34% ice).

(c) Snow: distribution of orientation angles (θ and ϕ) and shape are same as for wet ice. The density is a power-law function of equi-volume D as $\rho = 0.178*D^{-0.922}$ (Brandes et al. 2007).

The [*a*,*b*] of the frequency mapping are shown in Table 1.

Table 1: The [*a*,*b*] in Eq. 1 used for frequency scaling

		a_1	b_1	a_2	b_2
Rain(0°)		1.0591	0.3128	2.2478	0.0142
Rain (20°)	D_0≤1 mm	0.9942	-0.0960	2.3399	0.0339
	1<D_0≤1.5	1.0148	-0.4071	-	-
	1.5<D_0≤2	1.0451	-0.0238	-	-
	D_0>2	1.0026	2.2903	-	-
Wet Ice		0.9835	-1.4518	2.5524	-0.0037
Snow	D_0<1.47	0.9317	0.9385	3.2117	0
	D_0≥1.47	-	-	1.4107	0

Remark: "-" same as above

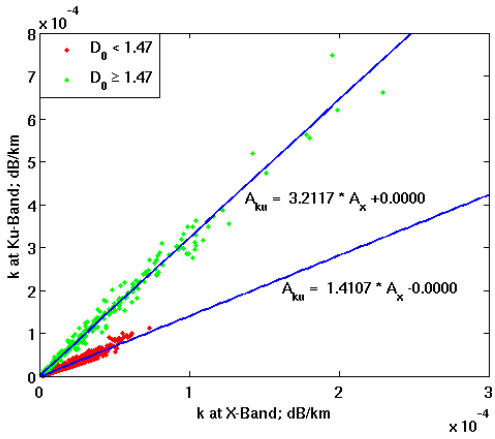

Figure 2: The scattering plot of *k* (A_h) at K_u-band vs. *k* at X-band. Note that frequency-convert separate into two group corresponding to the D_0.

As an example, Fig. 2 shows the k_{ku} verses k_x for snow. Note that the data separate into 2 branches based on the D_0 threshold of ~1.5 mm.

This is likely due to the fact that for snow the attenuation is caused by scattering effects (as opposed to absorption), and the green data branch in Fig. 2 for D_0 > 1.5 mm is likely due to Mie scattering effects. In practice, the snow attenuation is very small, $O(10^{-4})$, and does not contribute much to the PIA.

We use the same vertical structure model as Iguchi et al (2000). In convection, the mixed phase region is ±750 m off the freezing level (0℃). Above the mixed phase region, the hydrometers are assumed to be snow, and below the mixed phase region, it is rain. The [*a,b*] parameters in (1) are assumed to change linearly within the mixed phase region from snow at the top to rain at the bottom.

3. CASE STUDIES

With the help of Dr. Chuntao Liu of the University of Utah we identified 7 TRMM overpass events (from April to November 2008) within 100 km of the radar that were convective with substantial rain volumes. However, the X-band system was operational for only 2 of the overpass events. The first event was at 8 April 2008 that was ~ 40 km off the coast south east of Brisbane (coastal case but not 'open' ocean). The other example is over land to the W-NW of CP-2 on 5 November 2008.

3.1 Coastal Case: 8 April 2008

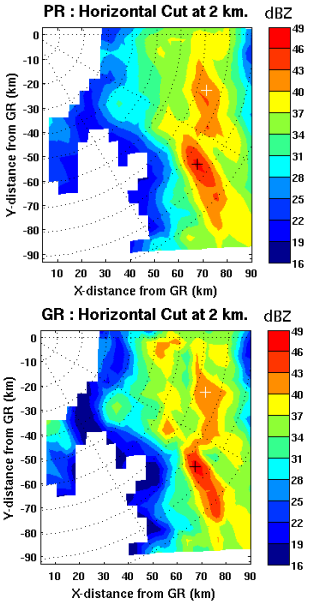

Figure 3: CAPPIs of 2A25 Z_c (upper panel) and CP-2 measured Z_h (S-band; bottom panel) at 2 km height. The "black +" is the most intense Z_h (~ 50 dBZ) and "white +" is the moderate Z_h (~40 dBZ). We will show the vertical profiles later.

Fig. 3 shows the CAPPIs of 2A25 Z_c (corrected radar reflectivity of PR; upper panel) and CP-2 measured S-band Z_h (bottom panel). Note that the alignment of 2 radars is excellent. Fig. 4 shows the vertical profile located at black "+" marked in Fig. 3. The upper panel of Fig. 4 show the radar reflectivity from (*a*) PR measured reflectivity in green line (Z_m; from 2A21), (*b*) CP-2 measured Z_h in red which is scaled from S-band to K_u-band, (*c*) PR-corrected reflectivity (PR-Z_c; from 2A25) in blue, and (*d*) PR reflectivity which has been corrected by CP-2 specific attenuation (CP2-Z_c; see the black line in bottom panel). The 0° C level is at 3 km from the Brisbane sounding data. The bottom panel show the specific attenuation from (*a*) CP-2 radar in black line (CP2-k; computed from DWR, and then, frequency scaled from X-band to K_u-band), (*b*) TRMM PR in blue line (PR-k; computed from $k=0.5*d/dr(\Delta Z)$ where $\Delta Z = Z_c - Z_m$), and (*c*) from the optimal estimation scheme which uses a radar model along with TMI data (MK-k: in purple) of Munchak and Kummerow (personal communication; henceforth referred to MK). It is obvious that CP2-*k* is higher than the PR-*k* below the freezing level and that the CP2-Z_c is in good agreement with CP-2 measured Z_h below the freezing level.

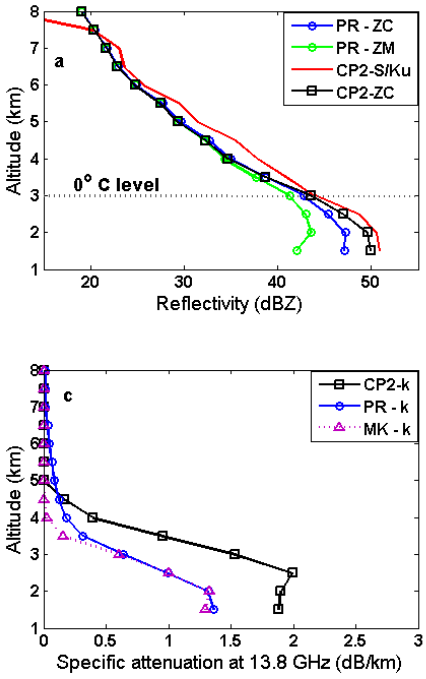

Figure 4: The vertical profiles of radar reflectivity (upper) and specific attenuation (bottom) from the 4X4 km grid box centered at the black "+" marker shown in Fig. 3.

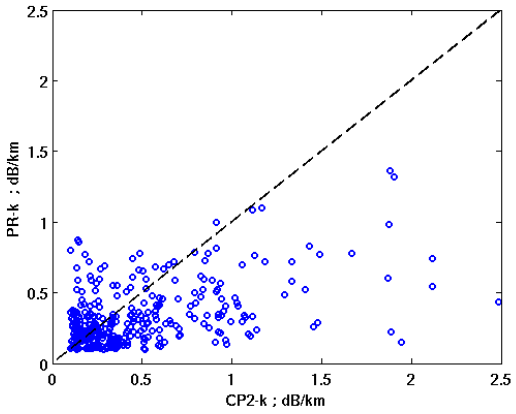

Figure 5: Scatter plot of CP2-*k* vs. PR-*k* from all pixels in z-cuts at 0.5,1,1.5 and 2 km heights. The threshold is 0.1 dB/km.

Fig. 5 shows the scatter plot of CP2-*k* versus PR-*k* from rain region (height ≤ 2 km) with 0.1 dB/km threshold. The mean of Δk is 0.15 dB/km, and the standard deviation is 0.36 dB/km where Δk is the CP2-*k* minus PR-*k*.

3.2 Over Land Case: 5 November 2008

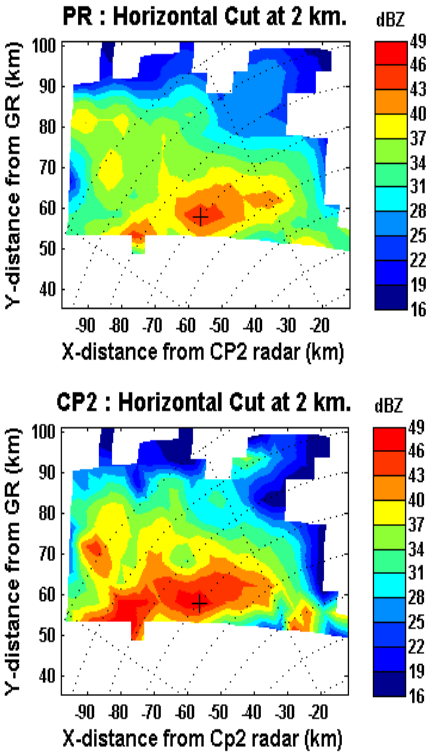

Figure 6: Same as Fig. 3 except from 5 November 2008.

Fig. 6 shows the CAPPIs of PR-Z_c (upper) and CP2-Z_h at 2 km height from 5 November 2008. Note that the alignment of these two radar reflectivities is not as good as the coastal case (see Fig. 3). Again, Fig. 7 shows the vertical profiles of radar reflectivity and specific attenuation located at the black "+" marker in Fig. 6. The CP2-*k* is 1 dB/km higher than PR-*k* at 2 km height. Similar to the coastal case, the CP2-Z_c agrees with CP-2 S/K_u-band Z_h below 3 km height.

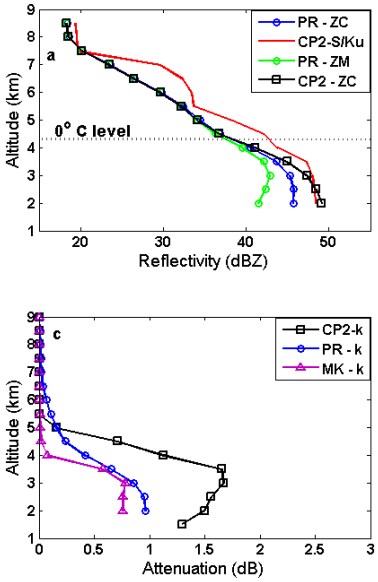

Figure 7: Same as in Fig. 4 except from 5 November 2008.

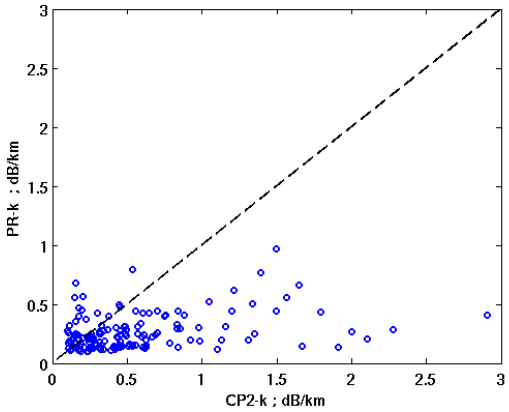

Figure 8: Same as in Fig. 5 except from 5 November 2008. Note that compared with coastal case, the PR-*k* is significantly under-estimated compared to the coastal case.

Finally, Fig. 8 shows the scatter plot of PR-*k* versus CP2-*k*. The mean of Δk is 0.3 dB/km and the standard deviation is 0.47 dB/km. Both cases (coastal and land) show that, comparing PR with CP-2, the PR-*k* is less than CP2-*k*, and the agreement of over the coastal case is better than over land. This is not unexpected as the SRT is more reliable over ocean than over land.

4. CONCLUSIONS

In this paper, we used the dual-wavelength technique to compute the specific attenuation from CP-2 radar data and compared with TRMM-overpass PR data. Two cases (coastal and land) have been analyzed. Both cases show that k from 2A25 is under-estimated compared with CP-2, though the coastal case is in better agreement than the over land case. The under-estimate of k (and *PIA*) will cause the TRMM hybrid method to under-estimate the ε_f. In terms of rain rate, it will also be under-estimated; in terms of DSD, it will underestimate N_w and overestimate D_0. Moreover, the comparison of CP-2 Z_h with CP2-Z_c agrees with each other well. This also implies that the k computed from *DWR* is reliable.

Clearly two events are not sufficient to draw firm conclusions, but the general feature of PR underestimate of R in convective rain is not in disagreement with other comparisons or observations. For example, Liao and Meneghini (2009) found from 9 years of R comparisons between the Melbourne WSR-88D and 2A25, that the PR-R 'near surface rain rate' systematically underestimates the WSR-88D 2A53 rain product for moderate-to-heavy rain. Their average underestimate was 19% but they note that, " ..the actual estimates of rain rate from the PR are expected to be worse than 19% in some ranges, such as in heavy rain. It is also noted that a negative bias in the PR estimates for convective rain is consistent with the results of the reflectivity comparisons in which it was found that the PR is about 1.6 dB smaller than the WSR". Their data from Melbourne, Florida should encompass both land and off the coast events.

Liu and Zipser (personal communication: see, trmm.chpc.utah.edu/2a12_land_anamolies_LZ.pdf) noted differences in 2A12 and 2A25 rain rates, the most notable over the Congo region where Version 6 of 2A25 rain rate strongly underestimates the 2A12 estimate (generally the trend for convective rain over land and in the afternoon). Similarly, Okamoto (personal communication) noted that 2A12 rain rates exceeded 2A25 rates by around 30-40% for every season over land and that 2A25 rainfall was less than the GPCC gage measurements over land quoting 7000 stations over a 9 year period. We are not suggesting that the 2A12 is superior than 2A25 over land, only that systematic underestimates of the 2A25 rain rates have been reported for deep convection over land and that correcting for this is the goal for Version 7. *A much larger set of TRMM overpass comparisons with CP2 ground radar, as proposed herein, would help validate Version 7 algorithms.*

ACKNOWLEDGEMENTS

This work was supported by the NASA Precipitation Measurement Mission (PMM) grants program to Colorado State University. The authors are grateful to the Centre for Australian Weather and Climate Research, Melbourne for use of the CP-2 radar. They also provided partial travel support to VNB to visit Brisbane and Melbourne in February 2008. Dr. Chuntao Liu of the University of Utah provided valuable guidance in selection of the TRMM overpass events. The authors acknowledge useful discussions with Prof. Kummerow and Joe Munchak of Colorado State University.

REFERENCES

Awaka, J., Y. Furuhama, M. Hoshiyama, and A. Nishitsuji, 1985: Model calculations of scattering properties of spherical bright-band particles made of composite dielectrics, *J. Radio Res. Lab.,* vol. **32**, 73-87.

Brandes, E.A., K. Ikeda, G. Zhang, M. Schönhuber, and R.M. Rasmussen, 2007: A statistical and physical description of hydrometeor distributions in Colorado snowstorms using a video disdrometer, *J. Appl. Meteor. and Climat*., vol. **46**, 634-650, 2007.

Bolen, S.M. and V. Chandrasekar, 2003: Methodology for aligning and comparing spaceborne radar and ground-based radar observations, *J. Atmos. Oceanic Techn.,* 20, 647–659.

Bringi, V.N. and M. Thurai, 2008: Preliminary assessment and analysis of the CP2 S&X band data, Internal report for the Centre for Australian Weather and Climate Research, Melbourne, AU.

Bringi, V.N., G. Huang, P.T. May, K. Glasson, and T.D. Keenan, 2009: The estimation of X-band attenuation due to wet ice in the mixed phase region of convective storm and correction of LDR at X-band using the CP-2 radar., Preprints, *34th Int. Conf. on Radar Meteor.,* Williamburg, VA, 11A.3.

Chandrasekar, V., K. Mubarak, and S. Lim, 2003: Estimation of raindrop size distribution from TRMM precipitation radar observations, *Proc. IGARSS,* Toulouse, France, 1712-1714.

Ferreira, F., P. Amayenc, S. Oury and J. Testud, 2001: Study and Tests of Improved Rain Estimates from the TRMM Precipitation Radar. *J Appl. Meteor.* Vol. **40**, 1878–1899

Hitschfeld, W., and J. Bordan, 1954: Errors inherent in the radar measurement of rainfall at attenuating wavelengths., *J. Meteor.,* Vol. **11**, 58-67.

Hubbert, J., and V.N. Bringi, 1995: An iterative filtering technique for the analysis of copolar differential phase and dual-frequency radar measurements, *J. Atmos. Oceanic Technol.,* Vol. **12**, 643-648.

Iguchi, T., T. Kozu, R. Meneghini, J. Awaka, and K. Okamoto, 2000: Rain-profiling algorithm for the TRMM Precipitation radar, *J. Appl. Meteor.*, vol. **39**, 2038-2052.

Liao, L. and R. Meneghini, 2009: Validation of TRMM precipitation radar through comparison of its multiyear measurements with ground-based radar, *J. Appl. Meteor. Climatol.,* 48, Issue 4, 804–817.

Meneghini, R., T. Iguchi, T. Kozu, L. Liao, K. Okamoto, J.A. Jones, and J. Kwiatkowski, 2000: Use of the surface reference technique for path attenuation estimates from the TRMM Precipitation radar, *J. Appl. Meteor.,* vol. **39**, 2053-2070.

Thurai, M., G. Huang, V.N. Bringi, W.L. Randeu, and M. Schönhuber, 2007: Drop shape, model comparisons, and calculations of polarimetric radar parameters in rain, *J. Atmos. Oceanic Technol.,* vol. **24**, 1019-1032.